

A Quantum Kinetic Solver: Theory, Structure and Simulation

Tian-Xing Hu^a, Jiong-Hang Liang^a, Dong Wu^{b,*}, Zheng-Mao Sheng^{a,**}

^a*Institute for Fusion Theory and Simulation, Department of Physics, Zhejiang University, Hangzhou 310027, China.*

^b*Key Laboratory for Laser Plasmas and School of Physics and Astronomy, Collaborative Innovation Center of IFSA, Shanghai Jiao Tong University, Shanghai 200240, China.*

Abstract

High-Energy-Density-Plasma differs from classical plasma in the follow two respects: (1) The statistical equilibrium become Fermi-Dirac-like instead of Maxwellian; (2) The quantum nature of single electron, i.e., the wave effect, has to be considered. The Wigner equation is the quantum version of Vlasov equation, the former is more general than the latter. However the solution of Wigner equation is non-trivial. Here we have adopted a hybrid splitting scheme in a Eulerian grid, where the x and v direction of the phase space are advanced by different methods. The hybrid scheme shows significant improvements when compared with the typical splitting scheme, especially when the non-linear interactions become serious. The linear results with temperature effect is tested, we found that the extra unstable region of two-stream instability is suppress by kinetic effect except when the quantum parameters are in a certain range. The quantum nonlinear Landau damping is also presented.

Keywords:

HEDP; Wigner Equation;

1 PROGRAM SUMMARY

2 **Program Title:** QUAKINS

3 **Programming language:** C++

4 **Nature of problem:** Wigner equation describes the behavior of quantum collisionless
5 plasmas just like the Vlasov equation describes the classical plasmas. Quakins provide a
6 general numerical solution of the Wigner equation efficiently, where a long-time nonlinear
7 simulation is also supported.

* dwu@sjtu.edu.cn

** zmscheng@zju.edu.cn

8 ***Solution method:*** *Solving the Vlasov/Wigner equation via splitting method.*

9 ***Restrictions:*** *Collisional and electromagnetic effects are not included.*

10

11

12 **1. Introduction**

13 In a kinetic theory, state of plasmas is indicated by a distribution function
14 $f(\mathbf{x}, \mathbf{v}, t)$, which evolves with time according to the famous Vlasov or Boltzmann
15 equation. Solving the Vlasov/Boltzmann equation is one of the most important
16 tasks for a plasma physicist. However, a nonlinear Boltzmann equation is almost im-
17 possible to solve analytically, numerical means are often needed. As a 6-dimension
18 phase space fluid (PSF), the numerical methods can be categorized into two types
19 analog to computational fluid dynamics: the Lagrangian and Euler method. In La-
20 grangian perspective, the PSF is marked by a huge amount of space point travelling
21 with corresponding velocity. Those points are called “markers” in magnetic fusion
22 literature and “marco-particles” or “clouds of particle” in the field of high density
23 plasma. This kind of method is known as the Particle-in-Cell (PIC) method. A ma-
24 jor defect of PIC is the inevitable noise caused by the Monte-Carlo process. On the
25 contrary, Euler methods are noiseless, but it is computationally unaffordable when
26 the dimension of the simulated space is higher than two.

27 In the field of High-Energy-Density-Plasmas (HEDP), traditional kinetic meth-
28 ods fail for the quantum effects become dominant. Many-body quantum mechanics
29 is one of the most popular approaches to deal with quantum plasmas [1], which
30 usually requires directly solving the many-body wave-function. However, it could
31 not produce dynamical results [2]. An alternative approach is the quantum kinetic
32 theory (QKT), which is essentially just a different form of many-body Schrödinger
33 equation. The governing equation of QKT is the quantum Vlasov equation, also
34 known as the Wigner equation [3]. Numerical methods solving classical phase space
35 problem, namely, solving the Vlasov or Boltzmann equation have been vastly in-
36 vestigated in the past decades. Hence the quantum effect can be introduced as a
37 correction to approximately describe a mesoscopic system. Furthermore, since the
38 phase-space-based method is a real time-dependent Hartree mean-field theory, it is
39 able to deal with dynamic correlations, i.e., collisions, among distribution functions
40 [2]. The collisional process are easily introduced into the phase-space framework by
41 simply add a collision term at the right-hand-side of kinetic equation, which can be
42 solved by directly solving [4], or Monte-Carlo relaxation method, depending on the
43 form of collision term.

44 To solve the nonlinear Wigner equation, Fourier spectrum method (FSM) [3] is
 45 often needed. However, in the nonlinear stage, the phase space calculated by FSM
 46 become unphysically chaotic. We thus adopt a combined method in this paper to
 47 remove this unphysical issues.

48 This paper is organized as follows. In section 2, the basic theory and numerical
 49 algorithms are introduced. We adopted a hybrid splitting scheme in the `quakins`
 50 code to solve the Wigner equation. The code structure is briefly introduced in section
 51 3. Results of `quakins` are presented in section 4, including both the classical and
 52 the quantum result of Landau damping and two-stream instability. Some riveting
 53 nonlinear phenomena are also presented.

54 2. Basic Theory and Methods

55 2.1. Quantum Kinetic Theory

In simple terms, the Wigner equation [?]]

$$\begin{aligned} \left(\frac{\partial}{\partial t} + \mathbf{v} \cdot \nabla \right) f(\mathbf{x}, \mathbf{v}, t) &= \frac{1}{i\mathcal{Q}} \int d\xi \int \frac{d\mathbf{v}'}{(2\pi\mathcal{Q})^3} \\ &\times e^{i(\mathbf{v}' - \mathbf{v}) \cdot \xi / \mathcal{Q}} \left[\phi \left(\mathbf{x} + \frac{\xi}{2} \right) - \phi \left(\mathbf{x} - \frac{\xi}{2} \right) \right] f(\mathbf{x}, \mathbf{v}', t) \end{aligned} \quad (1)$$

is just the quantum version of the electrostatic Vlasov equation:

$$\left(\frac{\partial}{\partial t} + \mathbf{v} \cdot \nabla - \nabla \phi \cdot \frac{\partial}{\partial \mathbf{v}} \right) f(\mathbf{x}, \mathbf{v}, t) = 0. \quad (2)$$

One can see that they are identical when $\phi(\mathbf{x})$ varying slowly in space. Here,

$$\mathcal{Q} = \frac{\hbar\omega_p}{2k_B T} \quad (3)$$

is the normalized Planck's constant, which, in quantum kinetic theory, measures the importance of quantum effect. Noticing that there is a intrinsic difference between Eq. (1) and Eq. (2): the definition of f in Eq. (1) is not a distribution function, i.e., a probability distribution, but

$$f(\mathbf{x}, \mathbf{v}, t) = \int d\xi e^{-im\mathbf{v} \cdot \xi / \hbar} \left\langle \Psi^\dagger \left(\mathbf{x} - \frac{\xi}{2} \right) \Psi \left(\mathbf{x} + \frac{\xi}{2} \right) \right\rangle, \quad (4)$$

56 where Ψ is the quantum field operator, and $\langle \dots \rangle$ stands for ensemble average. Eq.
 57 (4) is known as *the Wigner quasi-distribution function* [5]. The Wigner function

58 must not be interpreted as a probability distribution, because it can have negative
 59 values. In fact, this is the most significant difference between the quantum kinetic
 60 theory and traditional kinetic theory. Negative values imply the presence of quantum
 61 coherence in high-density plasmas.

62 2.2. Numerical Methods

63 The most common method for solving a Vlasov equation in Euler grids is to split
 64 a single calculating step into two parts [6], which are in x and v direction respectively.
 65 The flux balance method (FBM) [7] is commonly used when solving the Vlasov, while
 66 the Wigner equation can only be solved by Fourier spectrum method (FSM) [3] due
 67 to the cumbersome phase space integral. We adopt a novel scheme that combines
 68 these two methods, and the advantages of which will be presented in the following
 69 sections. Along with the Poisson equation solving process, a completed step of the
 70 main loop of the `quakins` code is in a leap-frog-like form.

71 2.2.1. Flux Balance Method

To solve a continuity equation

$$\frac{\partial f}{\partial t} + \frac{\partial}{\partial x}(vf) = 0, \quad (5)$$

one may discretize $f(x)$ into N uniform distributed grid point, and let

$$f_i = \frac{1}{\Delta x} \int_{x_{i-1/2}}^{x_{i+1/2}} f(x) dx. \quad (6)$$

In light of the nice property of Eq. (5), the integration in Eq. (6) is conserved along the characteristic curves. Hence,

$$\int_{x_{i-1/2}}^{x_{i+1/2}} f(x, t^b) dx = \int_{\mathcal{X}_{b \rightarrow a}(x_{i-1/2})}^{\mathcal{X}_{b \rightarrow a}(x_{i+1/2})} f(x, t^a) dx, \quad (7)$$

where $\mathcal{X}_{b \rightarrow a}$ maps a space location at time t^b to its whereabouts at time t^a along characteristic curve [7]. In this case $\mathcal{X}_{b \rightarrow a}(x) = x - v(t^b - t^a)$. Defining

$$\Phi_k^{ba} = \int_{\mathcal{X}_{b \rightarrow a}(x_k)}^{x_k} f(x, t^a) dx, \quad (8)$$

which is the total volume that flow through x_k point from t^a to t^b , then we have

$$f_i(t^b) \Delta x = f_i(t^a) \Delta x + \Phi_{i-1/2}^{ba} - \Phi_{i+1/2}^{ba}, \quad (9)$$

72 which is a perfect discretization of the continuity equation (5). Noticing that Eq.
 73 (9) indicate that the change in total volume in a single cell from t^a to t^b is equal
 74 to the volume flow in from left boundary($x_{i-1/2}$) minus the volume flow out from
 75 right boundary($x_{i+1/2}$). The flux integral of all the boundaries can then be evaluated
 76 independently:

$$\Phi_{i+\frac{1}{2}}(t^n) = \int_{x \in \alpha_{i+1/2}} f(t^n, x) dx + \begin{cases} \sum_{a=I+1}^i f_a^n \Delta x, & \text{while } v > 0 \\ - \sum_{a=i+1}^{I-1} f_a^n \Delta x, & \text{while } v < 0 \end{cases}. \quad (10)$$

77 In **quakins** code, the first integration term in Eq. 10 can be calculated by interpo-
 78 lation of any order of accuracy.

79 2.2.2. Fourier Spectrum Method

The flux balance method can easily handle a Vlasov equation but not the Wigner equation because of the cumbersome phase space integration term. However, it turn out that this term become more clear in Fourier space [3]:

$$\frac{\partial}{\partial t} f_\lambda(x, t) = \frac{e}{i\hbar} \left[\phi \left(x + \frac{\hbar\lambda}{2m} \right) - \phi \left(x - \frac{\hbar\lambda}{2m} \right) \right] f_\lambda(x, t). \quad (11)$$

Here, λ is the Fourier conjugate of velocity v . The solution of Eq. (11) is

$$f_\lambda(t) = f_\lambda(t - \Delta t) \exp \left\{ \frac{e}{i\hbar} \left[\phi \left(x + \frac{\hbar\lambda}{2m} \right) - \phi \left(x - \frac{\hbar\lambda}{2m} \right) \right] \Delta t \right\}. \quad (12)$$

Similarly, the x direction advance equation is in k -Fourier space:

$$f_k(t) = f_k(t - \Delta t) e^{ikv\Delta t}. \quad (13)$$

80 This implies that one can solve the Wigner function by means of Fourier spectrum
 81 method.

82 2.2.3. hybrid splitting Method

In **quakins**, we adopt a hybrid splitting method, in which, the x -direction is advance by FBM method while the v -direction the FSM method. Then a full step of the main loop is

$$\begin{aligned} f^*(x, v) &= f \left(x - v \frac{\Delta t}{2}, v, t - \Delta t \right), \\ \mathfrak{F}[f^{**}](\lambda) &= \mathfrak{F}[f^*](\lambda) e^{i\mathcal{E}(x)\lambda\Delta t}, \\ f(x, v, t) &= f^{**} \left(x - v \frac{\Delta t}{2}, v \right), \end{aligned} \quad (14)$$

where \mathfrak{F} stands for a Fourier transformation, and

$$\mathcal{E}(x) = \begin{cases} -\partial\phi/\partial x, & \text{while } \mathcal{Q} = 0, \\ [\phi(x + \mathcal{Q}\lambda/2) - \phi(x - \mathcal{Q}\lambda/2)]/\mathcal{Q}, & \text{otherwise.} \end{cases} \quad (15)$$

83 From Fig. 1 one can see that, the total energy, which equals to the sum of the
 84 electrostatic wave(ESW) energy ($\propto |E|^2$) and particle energy ($\propto \int v^2 f dv$), calculated
 85 by the pure FSM and hybrid method are both conserved. And, the linear stage of the
 86 ESW of these two Methods perfectly coincide, but disagreed in the nonlinear stage.
 87 Noticing that the two both predicted a sudden collapse of ESW in the nonlinear
 88 saturation stage, but the collapse time are discrepant. This collapse is actually a
 89 nonlinear side-band instability caused by mode-mode coupling [8], which indicates
 90 the broken of a Bernstein-Greene-Kruskal(BGK) equilibrium [9]. To see which mean
 91 is more reliable, we shall take a look at the phase space. In Fig. 2, where snap-shot
 92 of a typical BGK holes calculated by the two means respectively are presented, one
 can see that the FSM phase space is quite noisy, while the hybrid is fairly smooth.

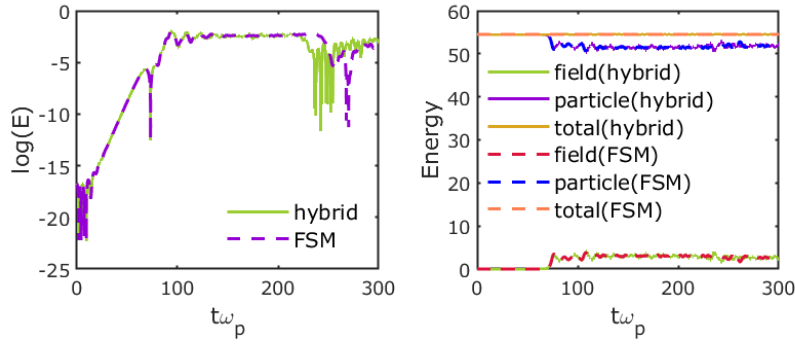


Figure 1: Electric field at a random position(left) and the energy of plasma and wave (right) of a typical two-stream instability.

93

94 2.2.4. Hypercollision Operator

95 As the simulation goes on, the ballistic term($\propto e^{ikvt}$) create a increasingly high
 96 wave-number of velocity space. In real world, this term will automatically fade away
 97 in light of phase mixing. However, in discrete phase space, the velocity space integral
 98 is replaced by a finite summation. As a result, the Fourier integral degrades to sum
 99 of Fourier series, hence a physical quantity become periodic in time. This is the
 100 so-called recurrence problem [6].

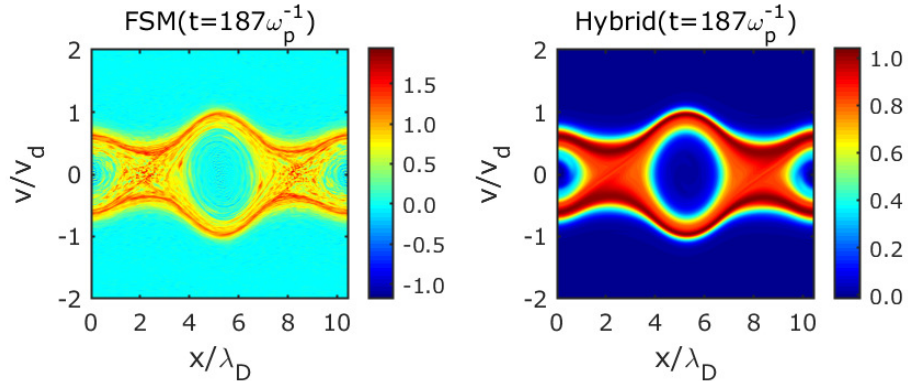


Figure 2: Snap-shot of two-stream instability at nonlinear phase simulated by pure fft method and hybrid method respectively, where $n_x = 200, n_v = 201, k = 0.6$.

We introduce a hypercollision operator [10]

$$C(f) = \nu_h \frac{\partial^4 f}{\partial v^4} \quad (16)$$

101 to cope with the recurrence problem.

102 3. Code Structure

103 The `quakins` (QUAntum KINetic Solver) code is developed in C++ language,
 104 and used for solving the 1d nonlinear Wigner/Poisson system in Euler grids with
 105 periodic boundary condition. We adopt the MPI parallelization scheme in order to
 106 do quick parameter scanning. The algorithm repository of `quakins` is designed to
 107 be easily expandable. The Poisson's equation solver and the free stream solver are
 108 two pure virtual interfaces, which allow one to enrich the algorithm repository via
 109 simply adding a subclass of the pure virtual base class (see Fig. 3).

110 4. Simulation Results

111 4.1. Classical Results($Q = 0$)

Landau damping is one of the most common kinetic phenomenon in plasma physics. Here we carry out the analytical continuation of the plasma dispersion function [11]

$$Z(\zeta) = i\sqrt{\pi}e^{-\zeta^2} [1 + \operatorname{erf}(i\zeta)] \quad (17)$$

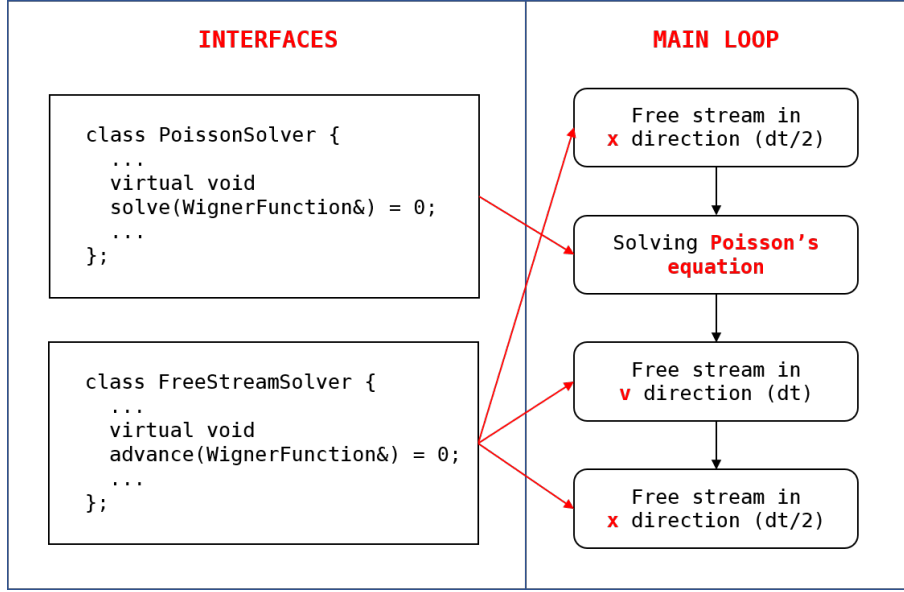


Figure 3: Quakins code as an API.

to calculate the exact solution of classical Landau damping (solid lines in Fig. 4(a)). The initial perturbation of the numerical result is of the form

$$f(x, v, 0) = f_0(v) [1 + A \cos(k_0 x)]. \quad (18)$$

To minimize unwanted nonlinear effects, we set $A = 10^{-3}$ for Landau damping. One can see from Fig. 4(a) that the numerical results perfectly coincide with the exact solution. Fig. 4(a) also shows the analytic solution obtained from Landau integral (the dash-lines), which is only valid in a very limited region ($k\lambda_D \ll 1$). Fig. 4(b) present the result of a typical two-stream instability. To the linear limit, the two-stream instability is not a kinetic effect, and the solid-lines in Fig. 4(b) is the solution to the reactive-type dispersion relation:

$$1 - \frac{\omega_p^2}{(\omega - kv_d/2)} - \frac{\omega_p^2}{(\omega + kv_d/2)} = 0. \quad (19)$$

112 In simulation, we initialized two nearly cold beams ($v_{th}/v_d = 0.05$) with opposite
 113 velocity ($v/v_d = \pm 0.5$), where the kinetic effects should be negligible. When the
 114 initial perturbation $A = 10^{-6}$, one can see that the simulation results do coincide
 115 with the analytical solution.

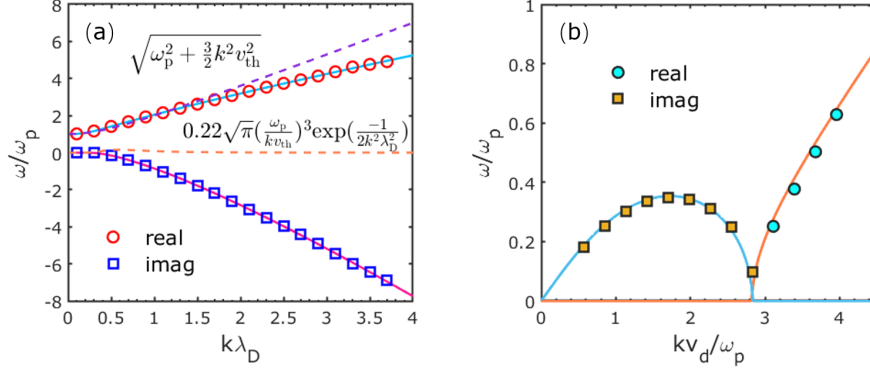


Figure 4: Linear growth rate of (a) Landau damping and (b) two-stream instability, where the solid lines are calculated by analytical equation, and the dash-lines are from Landau's approach.

116 4.2. Quantum Results ($\mathcal{Q} > 0$)

117 4.2.1. Landau Damping

When it comes to wave-particle interaction in kinetic theory, one needs to only consider the velocity component that parallel to the wave vector. Hence, after the integration over other two dimension, one obtain the one-dimensional Fermi-Dirac distribution

$$f(v) = \frac{3}{4} \frac{n_0}{v_F} \Theta \ln \left\{ 1 + \exp \left[\frac{1}{\Theta} \left(1 - \frac{v^2}{v_F^2} \right) \right] \right\}, \quad (20)$$

where $\Theta = k_B T / \epsilon_F$ is the degeneracy of a Fermi-Dirac system. Noticing that the degeneracy is related to the normalized Planck's constant \mathcal{Q} by

$$\Theta = 1.6813 \times 10^4 n^{-\frac{1}{6}} \mathcal{Q}^{-1}. \quad (21)$$

118 Hence, for a fixed electron density n , the shape of Fermi-Dirac distribution function
119 varies with \mathcal{Q} .

The dispersion relation presented in Fig. 5 is calculated under Maxwellian distribution, thus the degenerate effect is ignored. The dash-lines in the left panel of Fig. 5 stand for quantum fluid approximation [12], i.e.,

$$\omega^2 = \omega_p^2 + k \langle v \rangle^2 + \frac{\hbar^2 k^4}{4m_e^2}, \quad (22)$$

120 which, just like in the classical case, overestimated the real frequency. In Fig. 6, the
121 effect of Fermi-Dirac statistics are included. We calculated the dispersion relation
122 with $\Theta = 0.2, 0.5$ and 2 respectively. As can be seen, the shape of the distribution
123 function has a significant effect on the dispersion relation.

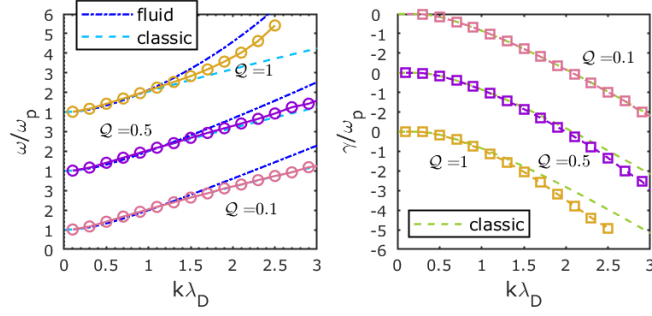


Figure 5: quantum Landau Damping with varying Q .

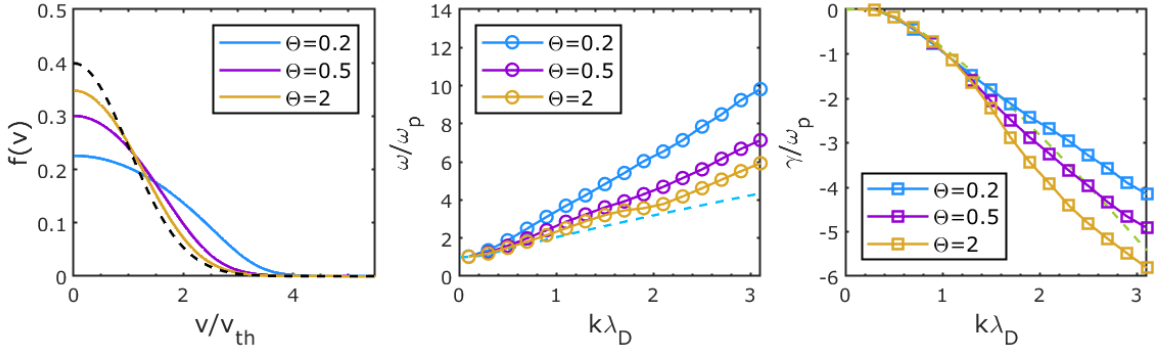


Figure 6: Quantum Landau Damping with varying $Theta$. The first panel is the shape of 1d Fermi-Dirac distribution, where the dashed-line represents the Maxwellian distribution.

124 4.2.2. Two-stream Instability

In quantum degenerate plasma, two-stream instability behave differently because of the Fermi pressure and the quantum wave effect [13, 14, 15, 16]. When the relative drift velocity of the two streams v_d is much larger than the Fermi velocity v_F or the thermal velocity v_{th} in non-degenerate plasma, it is reasonable to replace the distribution function by two counter-streaming δ -functions with velocity difference v_d . Since the kinetic effect is ignored, a reactive-type dispersion relation is obtained:

$$1 - \frac{\omega_{p1}^2}{(\omega - kv_1)^2 - \omega_k^2} - \frac{\omega_{p2}^2}{(\omega - kv_2)^2 - \omega_k^2} = 0, \quad (23)$$

where $\omega_k = \hbar k^2/2m_e$ is the quantum shift caused by diffraction and refraction of electrons. Let $v_d = v_1 - v_2$, $\omega_1^2 = \omega_2^2 = \omega_p^2/2$, and $v_1 + v_2 = 0$, we have

$$\omega^2 = \frac{\omega_p^2}{2} \left(1 + 2\tilde{k}^2 + 2H^2\tilde{k}^4 \pm \sqrt{1 + 8\tilde{k}^2 + 16H^2\tilde{k}^6} \right), \quad (24)$$

125 where $H = 2\hbar\omega_p/mv_d^2$, and $\tilde{k} = kv_d/2\omega_p$ is the normalized wave number. The plus
 126 sign gives a trivial solution since the frequency is always real. The imaginary part
 127 of roots with minus sign are plotted in Fig. 7, from which one can see that as H
 128 increases, there is an additional unstable bubble emerges at high- k and then merges
 129 with the original bubble as H further increases. When $H = 0$, the bubble is located
 130 at infinite- k . This additional unstable bubble would be better understood if the
 131 electromagnetic effect were considered [13]. Generally, an instability with such high
 132 value of wave number often suffers very strong Landau damping and being difficult
 133 to really grow up.

134 We thus conducted a simulation at $H \simeq 0.5$, while the two instability bubble are
 135 at the edge of merging. The temperature of the two beams are both $0.05v_d$, which
 136 corresponds to a low temperature system. The results are presented in right panel
 137 of Fig. 7. When $H = 0.48$, the unstable mode in the outer bubble is suppress by
 138 Landau damping albeit with such low temperature. When $H = 0.52$, where the
 139 outer bubble is attached to the main unstable bubble, and a larger unstable region is
 140 formed. The numerical result coincide with the theoretical result up to $k = 4\omega_p/v_d$
 141 while the remaining part is again suppressed by Landau damping. Be that as it may,
 142 the unstable region of QTS is still almost doubled when compared to the CTS (see
 143 Fig. 4).

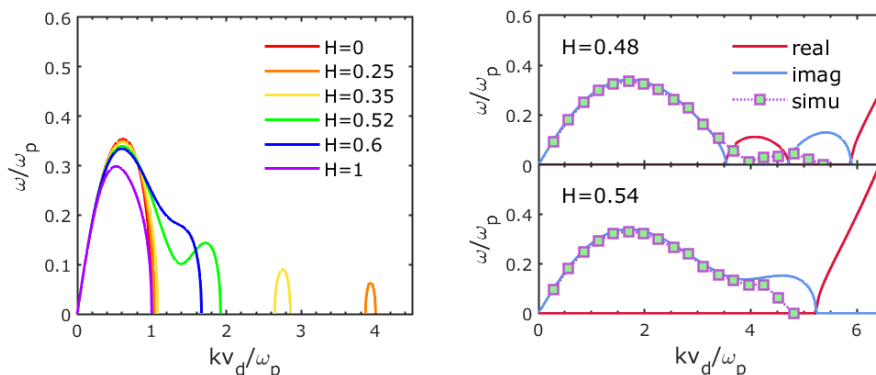


Figure 7: quantum two-stream instability.

144 *4.3. Nonlinear Effects*

In classical plasmas, a strong electrostatic perturbation can not be completely removed by Landau damping because of nonlinear effect, i.e., the particle trapping process. However, in a high-density-plasma, quantum tunneling effect prevent particles from being trapped by an electrostatic trough when the relation [17]

$$\frac{\hbar k}{m} \gtrsim \frac{\omega_p}{k} \sqrt{A} \quad (25)$$

145 is satisfied. More specifically, as is pointed out by the author of Ref. [18], there
 146 exists two time scales that determine the nonlinear behavior: the bounce period
 147 $t_B = 2\pi/\omega_B$, where ω_B is the bounce frequency of electrons, and the quantum time
 148 scale $t_Q = 2m/\hbar k^2$. When $t_Q \ll t_B$, the nonlinear trapping is suppressed, and when
 149 $t_Q \gg t_B$, the quantum result reduce to classical.

150 We then set $A = 0.06$ to initial a Landau damping with $Q = 0$ and 1 respectively.
 151 One can see from Fig. 8 that, when $k\lambda_D \simeq 0.6$, $t_Q \ll t_B$ is satisfied, the nonlinear
 152 trapping does be suppressed with no residue left. However, when $k\lambda_D \simeq 0.4$, where
 153 t_Q is just slightly less than t_B , the quantum result resembles the classical. The
 154 nonlinear effect is still evident. If we take a look at the snap-shot of phase space
 155 (additional panel in Fig. 8) at $t\omega_p = 52$, where the trapped electrons are in their first
 156 bounce period, we find that the resonant island of the quantum plasma, where the
 157 negative value indicates the quantum recoil, behaves very differently than its classical
 158 counterpart, albert the evolution of electric field nearly coincides. This implies that
 159 the quantum recoil phenomenon may not be as significant as the theoretical analysis
 160 has predicted.

161 **5. Summary**

162 In this paper, we adopt a hybrid splitting method to solve the Wigner equation,
 163 the accuracy of which is benchmarked by analytical linear theory. We have re-
 164 investigated the two famous phenomena in plasma physics: Landau damping and
 165 two-stream instability. The result shows that the Landau damping is much stronger
 166 in quantum plasmas than in classical plasma for two reasons: the quantum wave
 167 effect and the Fermi pressure. As to quantum two-stream instability, we find that
 168 the extra short-wave-length instability resulted by quantum recoil effect is suppress
 169 by strong Landau damping even with nearly zero temperature. And only exist when
 170 it is closely located at the original unstable region, which happens when $H \simeq 0.5$. In
 171 the nonlinear region, we conclude that the quantum recoil effect may not be as that
 172 important as the prediction of theoretical analysis.

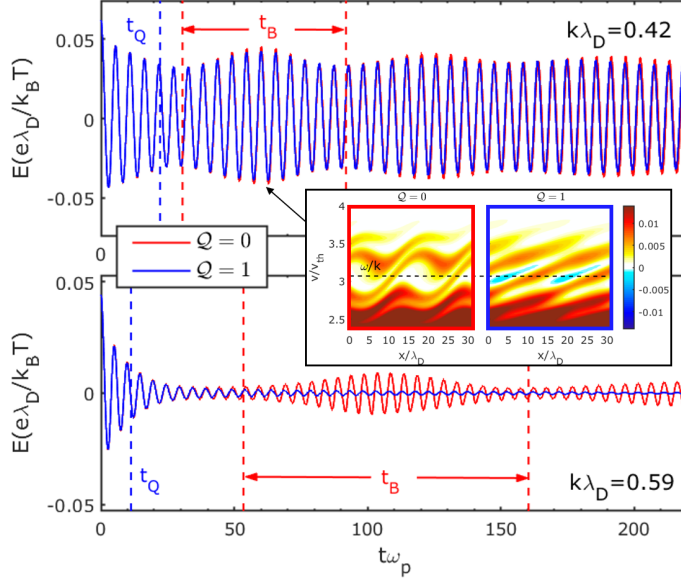


Figure 8: Nonlinear Landau Damping.

173 6. Acknowledgements

174 This work was supported by National Natural Science Foundation of China
 175 11875235 and 61627901.

176 References

- 177 [1] T. Dornheim, S. Groth, M. Bonitz, The uniform electron gas at warm dense
 178 matter conditions, *Physics Reports* 744 (2018) 1–86.
- 179 [2] G. Manfredi, P.-A. Hervieux, J. Hurst, Phase-space modeling of solid-state plas-
 180 mas, *Reviews of Modern Plasma Physics* 3 (1) (2019) 1–55.
- 181 [3] N.-D. Suh, M. R. Feix, P. Bertrand, Numerical simulation of the quantum
 182 liouville-poisson system, *Journal of Computational Physics* 94 (2) (1991) 403–
 183 418.
- 184 [4] J. Daligault, On the quantum landau collision operator and electron collisions
 185 in dense plasmas, *Physics of Plasmas* 23 (3) (2016) 032706.

- 186 [5] G. Manfredi, P.-A. Hervieux, J. Hurst, Phase-space modeling of solid-state plas-
187 mas, *Reviews of Modern Plasma Physics* 3 (1) (2019) 13.
- 188 [6] C.-Z. Cheng, G. Knorr, The integration of the vlasov equation in configuration
189 space, *Journal of Computational Physics* 22 (3) (1976) 330–351.
- 190 [7] F. Filbet, E. Sonnendrücker, P. Bertrand, Conservative numerical schemes for
191 the vlasov equation, *Journal of Computational Physics* 172 (1) (2001) 166–187.
- 192 [8] V. E. Zakharov, Collapse of langmuir waves, *Soviet Physics JETP* 35 (5) (1972)
193 908–914.
- 194 [9] I. B. Bernstein, J. M. Greene, M. D. Kruskal, Exact nonlinear plasma oscilla-
195 tions, *Physical Review* 108 (3) (1957) 546.
- 196 [10] T. Dannert, F. Jenko, Vlasov simulation of kinetic shear alfvén waves, *Computer
197 physics communications* 163 (2) (2004) 67–78.
- 198 [11] H.-S. Xie, Generalized plasma dispersion function: One-solve-all treatment, vi-
199 sualizations, and application to landau damping, *Physics of Plasmas* 20 (9)
200 (2013) 092125.
- 201 [12] G. Manfredi, F. Haas, Self-consistent fluid model for a quantum electron gas,
202 *Physical Review B* 64 (7) (2001) 075316.
- 203 [13] A. Bret, F. Haas, Connection between the two branches of the quantum two-
204 stream instability across the k space, *Physics of Plasmas* 17 (5) (2010) 052101.
- 205 [14] S. Son, Two-stream instabilities in degenerate quantum plasmas, *Physics Letters
206 A* 378 (34) (2014) 2505–2508.
- 207 [15] F. Haas, B. Eliasson, A new two-stream instability mode in magnetized quantum
208 plasma, *Physica Scripta* 90 (8) (2015) 088005.
- 209 [16] J.-H. Liang, T.-X. Hu, D. Wu, Z.-M. Sheng, Kinetic study of quantum two-
210 stream instability by wigner approach, *Physical Review E* 103 (3) (2021) 033207.
- 211 [17] G. Manfredi, How to model quantum plasmas, *Fields Institute Communications*
212 46 (2005) 263–287.
- 213 [18] J. Daligault, Landau damping and the onset of particle trapping in quantum
214 plasmas, *Physics of Plasmas* 21 (4) (2014) 040701.